HHS Public Access

Author manuscript

Small. Author manuscript; available in PMC 2019 February 26.

Published in final edited form as:

Small. 2010 May 21; 6(10): 1092–1095. doi:10.1002/smll.201000151.

Peptide-Nanotube Biochips for Label-Free Detection of Multiple Pathogens

Dr. Roberto de la Rica[*],
Department of Chemistry and Biochemistry, Hunter College, City University of New York, 695 Park Avenue, New York, NY 10065 (USA)

Christophe Pejoux,
Department of Chemistry and Biochemistry, Hunter College, City University of New York, 695 Park Avenue, New York, NY 10065 (USA)

Dr. Cesar Fernandez-Sanchez,
Department of Micro- and Nanosystems Instituto de Microelectronica de Barcelona, IMB-CNM, CSIC Campus UAB, 08193 Bellaterra (Spain)

Dr. Antonio Baldi, and
Department of Micro- and Nanosystems Instituto de Microelectronica de Barcelona, IMB-CNM, CSIC Campus UAB, 08193 Bellaterra (Spain)

Prof. Hiroshi Matsui
Department of Chemistry and Biochemistry, Hunter College, City University of New York, 695 Park Avenue, New York, NY 10065 (USA)

Keywords

arrays; bionanotechnology; bacteria; electrochemistry; sensors

Microarray technologies that integrate multiple high-density DNA and protein chips are revolutionizing the genomics and proteomics fields by facilitating the multiplexed detection of biomarkers on a single platform.[1–5] In the field of bacteria detection, a microarray of sensors could determine the absence of multiple pathogenic strains in a sample, a key factor to avoid infection.[6–8] However, the detection of pathogens imposes other restrictions: pathogen detection must be fast and sensitive to determine the presence of hazardous microorganisms in low numbers before they grow and become a severe health threat due to the rapid growth of microorganisms. The robust in-field detection of pathogens is also desirable to lower the risk of infection and hence miniaturized multisensors fully integrated with signal-processing circuits will be extremely useful. Furthermore, a reusable sensor chip with a simple washing procedure is critical to make such a compact device cost effective for its widespread application as a point-of-care sensor.

[*] roberto.delarica@gmail.com; hmatsui@hunter.cuny.edu.

Supporting Information is available on the WWW under http://www.small-journal.com or from the author.

To score highly in these requirements, we previously introduced the peptide-nanotube biochip for the label-free detection of virus.[9] In this biochip, antibody-conjugated peptide nanotubes were positioned at the gap between electrodes and the binding event between virus and nanotubes generated the impedimetric signal for pathogen detection. While this biochip can detect virus at a concentration of 100cfu mL^{-1} or higher, reuse of the sensor for multiple measurements is not straightforward due to the strong interaction between pathogens and antibodies on the peptide nanotube. In this Communication, we report the development of novel peptide-nanotube-based bacterial multisensor chips that do not require the preimmobilization of these nanotubes on electrodes and are therefore totally reusable. In this detection scheme, as antibody-conjugated peptide nanotubes agglutinate the cells in solution via specific biorecognition, the bacteria–nanotube complexes sediment quickly onto the surface of the transducer and the presence of the insulating cells changes the distribution of the electric-field lines and currents to increase the impedance at high frequency (Figure 1). In contrast, peptide nanotubes modified with nonspecific antibodies do not agglutinate the pathogens, thus resulting in a smaller variation of the impedance with time. Since this nanotube is not immobilized on the electrode, the bacteria– nanotube complex can be washed out easily by gently rinsing with water. The key sensing feature of this robust pathogen-detection scheme with reusable multisensory chips is achieved by the characteristic alternating current (AC) field impedimetric transduction mechanism and the use of circulating nonconductive peptide nanotubes as pathogen catchers. AC probes can detect the nonconductive bacteria–nanotube complexes without fixing the nanotubes firmly on the electrodes. In conventional immunosensor designs based on the use of conductive nanowires, the nonreversible nature of the antibody–pathogen interaction is problematic for the cleaning and reuse of the devices and the requirement of intimate contact between the nanowire and the electrode to transduce the signal can affect the reproducibility among different sensor chips due to variability of the contact resistance.[10–14] However, in our sensor design, the AC current is transmitted through the solution and not through the nanotubes and therefore intimate contact between the tubes and the electrodes is not necessary to transduce the signal.[9,15,16] The nanotubes are especially well suited for this application because the hollow structure of the nanotubes makes them transparent to the electric field and, consequently, decreasing the signal of the blank leads the sensitivity of the sensor being maximized. In addition, because the biorecognition events occur in the solution and not at the transducer surface, the sensors can be easily reused by washing existing cells and peptide nanotubes away with a simple rinsing procedure (Figures S1-S5 in the Supporting Information). Using this fully reusable electronic sensor chip, *E. coli* and *S. typhi* cells were successfully detected in the range from 10^2 to 10^4 cells within one hour, which makes the proposed detection platform suitable for the rapid detection of multiple pathogens.

In the proposed pathogen biochip, the specific recognition between antibody nanotubes and pathogens is a key factor to detect multiple bacterial strains simultaneously. To demonstrate the specific recognition of a bacterial strain by peptide nanotubes, the bindings of *E. coli* cells to both anti-*E. coli* coated peptide nanotubes (with affinity for *E. coli*) and rabbit-IgG-coated peptide nanotubes (with no affinity for *E. coli*) were compared. After mixing with a solution containing *E. coli* cells for one hour, anti-*E. coli* nanotubes recognized and

agglutinated *E. coli* cells (Figure 2c), whereas rabbit-IgG-conjugated peptide nanotubes did not recognize the cells with the same procedure, as shown in Figure 2e. These results demonstrate that antibody nanotubes interact specifically with a particular bacterial strain via biomolecular recognition.

When antibody-modified nanotubes bind pathogens, the resulting nanotube–bacteria complexes sediment faster on the transducer due to their increased total mass and generate the impedimetric signal via perturbation of the AC field by these insulating objects (Figure 2a). To demonstrate this hypothesis, a solution containing the complexes in Figure 2c was spotted onto one transducer of the microarray and the real part of the impedance at 316 kHz was measured with time to detect the presence of the complexes. At this frequency cells can be considered as purely insulating objects that deviate the path of the electric-field lines and currents[15] and the interdigitated transducer can monitor the resulting perturbations of the AC field sensitively[17] (see Sections S3 and S4 in the Supporting Information). As shown in Figure 2d, the agglutinated bacteria induce a large variation of Z' with time, whereas, in Figure 2f, the nonagglutinated bacteria do not sediment fast enough to increase Z' significantly. These results demonstrate the proposed transduction mechanism that measuring Z' at high frequency as the bacteria fall onto the transducers can detect the presence of pathogens after the agglutination by specific antibody nanotubes. Moreover, since the nanotubes modified with rabbit IgG generate a much smaller variation of Z' they can be used in control experiments to subtract nonspecific contributions to the signal, including temperature drift, parasitic components of the electric circuit, and nonspecific adsorption of the bacteria to the nanotubes. Remarkably, this experiment was repeated at least twenty times by simply rinsing the transducer for 10 s with deionized water and no nanotube–bacteria complexes were found on the surface (Figures S1-S5); the variation of the performance of the sensor after each washing step was found to be less than 5% (Section S2 in the Supporting Information), demonstrating the reusability of this pathogen biochip for bacteria detection.

After validating the specific detection of a particular bacterial strain with antibody nanotubes, the proof of concept of the multiplexed detection of pathogens was demonstrated by assaying two model bacteria, *E. coli* and *S. typhi*, at different concentrations with the peptide-nanotube biochip. The variation of the sensitivity among the transducers was observed to be less than 5% and therefore any transducer on the chip could be used indistinctively for the impedimetric detection of bacteria (see Section S2 in the Supporting Information). After samples containing four different concentrations of either *E. coli* or *S. typhi* were prepared (0, 10^2, 10^3, and 10^4 cells), each bacteria solution was mixed with either antipathogen nanotubes or control nanotubes for one hour. Every immunoassay was repeated twice, yielding a total of 32 measurements on the microarray. After subtracting the signal of the control to remove the nonspecific contributions, a variation of Z' with bacterial concentration was observed, as shown in Figure 3a. In this figure, $\Delta Z'$ increases more rapidly as the number of *E. coli* cells increases because more cells are agglutinated via biorecognition with the anti-*E. coli* nanotubes and the increased mass of the bacteria–nanotube complexes induces a fast sedimentation on the transducers to increase Z', as discussed in Figure 2. While these plots contain valuable information for specialists, the readout could become more accessible for nonexpert users if converted to a visual output,

especially in point-of-care applications. To compare the results of different bacterial strains and concentrations visually, $\Delta Z'$ at 15-s detection time in Figure 3a was converted into color charts, whose intensity is directly proportional to the amount of pathogens in the sample. In Figure 3b, both *E. coli* and *S. thyphi* generate signals that are easily associated with the concentrations of pathogens in the sample, therefore validating the effectiveness of the color chart approach for the rapid determination of pathogens in the low number. Since the dynamic range of the sensor, from 10^2 to 10^4 cells, is well below the minimum infective dose for the pathogenic strains of *E. coli* and *S. typhi* as well as for most foodborne pathogens,[18] the peptide-nanotube biochip is adequate for the early detection of multiple pathogens, a key factor to avoid infection.

In conclusion, the peptide-nanotube biochip features multiplexed detection capability and cost-effective reusability with outstanding sensitivity, which can be easily integrated with the circuitry. The detection strategy involves the agglutination of bacteria with nonconductive antibody-conjugated peptide nanotubes, whose fast sedimentation induces an increase of impedance at high frequency on transducers. By converting the signal to color charts, the presence and relative amount of multiple pathogens can be estimated easily and quickly, therefore emphasizing the suitability of this approach for infield measurements.

Experimental Section

Fabrication of the array of electrodes was carried out in a microfabrication clean room using common deposition and patterning techniques. Fabrication started with the deposition of a triple layer of Ti/Ni/Au (500Å/500Å/500Å) on a 500-μm-thick Pyrex wafer. After the metal layers were patterned with standard photolithography and wet etching of the metals, a 1-μm-thick silicon oxide passivation coating was deposited and patterned. Finally, the passivation layer was removed from the pads and from the interdigitated area with a second photolithography step and oxide dry etching. The peptide nanotubes were prepared by self-assembly from the bolaamphiphilic peptide monomer bis(N-a-amidoglycylglycine)-1,7-heptane dicarboxylate and used as templates for the immobilization of antibodies as reported previously.[19,20,9] To obtain antibody nanotubes, after centrifuging 1 mL of the peptide-nanotube solution at 14000rpm for 1h, the resulting pellet was suspended in 100 μL of phosphate buffer (PB, $1m_M$, pH 7) containing either anti-*E. coli* (goat polyclonal, 0.1 mg mL^{-1}, Abcam), anti-*S. typhi* (rabbit polyclonal, $0.1mgmL^{-1}$, Abcam), or IgG from rabbit serum (0.1 mg mL^{-1}, Sigma) overnight. Then, 500 μL of bovine serum albumin (BSA, 10 mg mL^{-1}) were added for 1h to block free adsorption sites on the tubes and the nanotubes were washed once with PB by centrifugation. After mixing 10mL of antibody nanotubes with 10 μL of bacteria solutions in PB with different concentrations for 1h, 1 μL of the resulting nanotube–bacteria adducts were spotted on each transducer and Z' at 316kHz was measured with a 1260 Solartron Impedance Analyzer by applying a peak-to-peak excitation voltage of 10mV. The x axis in Figure 3 shows the number of cells in the 10mL solution. In Figure 3b, Z' at 15-s sedimentation time of bacteria–nanotube complexes was converted into a color code by calculating the percentage variation of this parameter with respect to the maximum signal and tuning the brightness of the spot accordingly. Scanning electron microscopy (SEM) images were taken with a Zeiss Supra 55VP microscope by using an acceleration

voltage of 0.5kV after depositing the samples onto porous membranes (0.1-μm-diameter pore size, Whatman) and coating them with carbon.

Supplementary Material

Refer to Web version on PubMed Central for supplementary material.

Acknowledgments

This work was supported by the National Science Foundation (sensor fabrication, biological materials) under Award No. ECCS-082390 and by the U.S. Department of Energy, Office of Basic Energy Sciences, Division of Materials Sciences and Engineering (AC impedance analysis) under Award No. DE-FG-02-01ER45935. Hunter College infrastructure is supported by the National Institutes of Health, the RCMI program (G12-RR003037-245476). R.R. acknowledges a postdoctoral fellowship from the Spanish Ministerio de Ciencia e Innovacio´n and Fundación Española para la Ciencia y la Tecnología.

References

[1]. Gresham D, Dunham MJ, Botstein D, *Nat. Rev. Genet.* 2008, 9, 291–302. [PubMed: 18347592]

[2]. Fan R, Vermesh O, Srivastava A, Yen BKH, Qin LD, Ahmad H, Kwong GA, Liu CC, Gould J, Hood L, Heath JR, *Nat. Biotechnol.* 2008, 26, 1373–1378. [PubMed: 19029914]

[3]. Zheng GF, Patolsky F, Cui Y, Wang WU, Lieber CM, *Nat. Biotechnol.* 2005, 10, 1294–1301.

[4]. Jonkheijm P, Weinrich D, Schroder H, Niemeyer CM, Waldmann H, *Angew. Chem. Int. Ed.* 2008, 50, 9618–9647.

[5]. Wilson DS, Nock S, *Angew. Chem. Int. Ed.* 2003, 42, 494.

[6]. Pedrero M, Campuzano S, Pingarron JM, Sensors 2009, 9, 5503. [PubMed: 22346711]

[7]. Wang C, Irudayaraj J, Small 2008, 4, 2204–2208. [PubMed: 19003819]

[8]. Phillips RL, Miranda OR, You CC, Rotello VM, Bunz UHF, *Angew. Chem. Int. Ed.* 2008, 47, 2590–2594.

[9]. de la Rica R, Mendoza E, Lechuga LM, Matsui H, *Angew. Chem. Int. Ed.* 2008, 47, 9752–9755.

[10]. Stern E, Klemic JF, Routenberg DA, Wyrembak PN, Turner-Evans DB, Hamilton AD, LaVan DA, Fahmy TM, Reed MA, Nature 2007, 445, 519–522. [PubMed: 17268465]

[11]. Wang RH, Ruan CM, Kanayeva D, Lassiter K, Li YB, *Nano Lett.* 2008, 8, 2625–2631. [PubMed: 18715043]

[12]. Patolsky F, Zheng GF, Hayden O, Lakadamyali M, Zhuang XW, Lieber CM, Proc. Natl. Acad. Sci. USA 2004, 101, 14017–14022. [PubMed: 15365183]

[13]. Yemini M, Reches M, Gazit E, Rishpon J, Anal. Chem. 2005, 77, 5155–55159. [PubMed: 16097753]

[14]. Yemini M, Reches M, Rishpon J, Gazit E, *Nano Lett.* 2005, 5, 183–186. [PubMed: 15792436]

[15]. de la Rica R, Baldi A, Fernandez-Sanchez C, Matsui H, *Anal. Chem.* 2009, 81, 3830–3835. [PubMed: 19334738]

[16]. a) Beck JD, Shang L, Marcus MS, Hamers RJ, *Nano Lett.* 2005, 5, 777–781; [PubMed: 15826127] b) Beck JD, Shang L, Li B, Marcus MS, Hamers RJ, Anal. Chem 2008, 80, 3757–3761; [PubMed: 18407615] c) de la Rica R, Baldi A, Fernandez-Sanchez C, Matsui H, Anal. Chem 2009, 81, 7732–7736. [PubMed: 19746997]

[17]. de la Rica R, Fernandez-Sanchez C, Baldi A, *Appl. Phys. Lett.* 2007, 90, 174104.

[18]. Kothary MH, Babu US, Food Safety J 2001, 21, 49–73.

[19]. Kogiso M, Ohnishi S, Yase K, Masuda M, Shimizu T, Langmuir 1998, 14, 4978–4986.

[20]. Matsui H, Gologan B, J. Phys. Chem. B 2000, 104, 3383–3386.

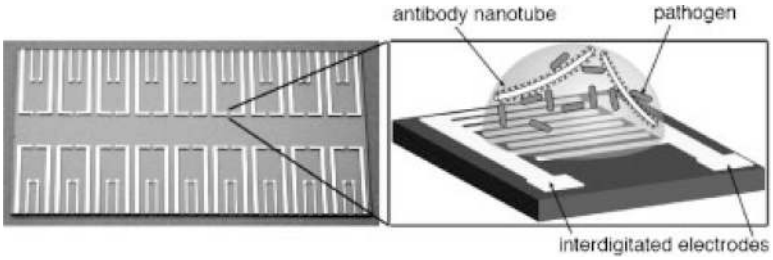

Figure 1.

Peptide-nanotube biochip. Left: detection platform consisting of 36 interdigitated transducers; right: on each transducer, antibody-modified peptide nanotubes recognize and bind cells to generate an impedimetric signal for pathogen detection via fast sedimentation of these complexes onto the transducer.

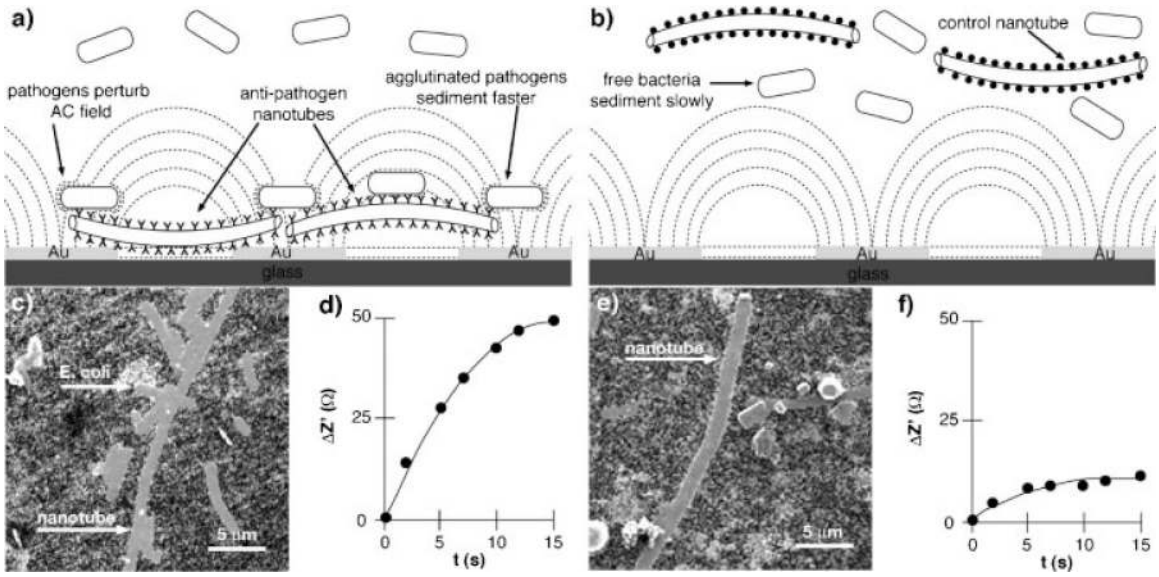

Figure 2.

Label-free detection of pathogens with antibody-modified peptide nanotubes. a) Bacteria agglutinated by the interaction with antibodies on peptide nanotubes sediment quickly and the increased number of the insulating cells on the transducer via the sedimentation increases the impedance at 316 kHz. b) Controlnanotubes modified with rabbit IgG that do not interact specifically with *E. coli* do not sediment these cells fast enough to generate the impedance signal. c) SEM image of *E. coli* agglutinated by anti-*E. coli* nanotubes. d) Increase of the real part of the impedance ($Z^{'}$) at 316 KHz with time due to the fast sediment at ion of bacteria–nanotube complexes in (c) on the transducer. e) SEM image of control nanotube modified with rabbit IgG that does not interact with *E. coli*. f) A significantly smaller $Z^{'}$ change as compared to (d) when *E. coli* cells are mixed with control

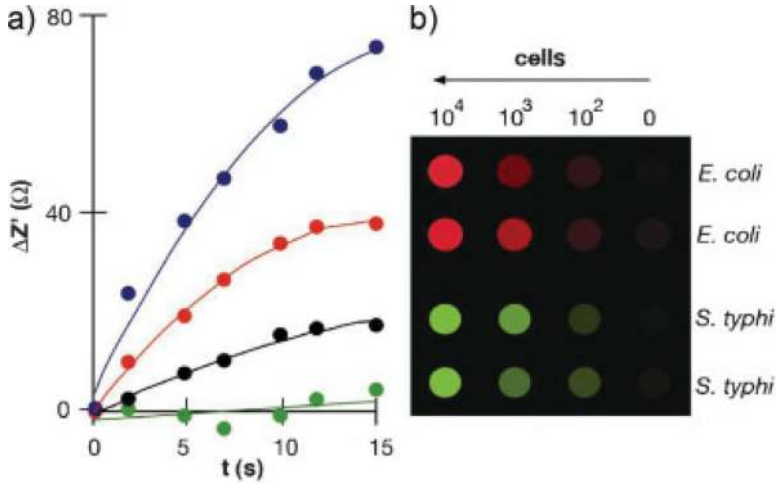

Figure 3.

Multiplexed detection of pathogens with the peptide-nanotube biochip. a) Variation of the real part of the impedance (Z') generated by 10^4 cells (blue), 10^3 (red), 10^2 cells (black), and 0 cells (green) of E. coli. b) Z' at 15 s was converted into a color chart for *E. coli* and *S. typhi* as duplicates on the array (see also Figure S9 online).